Journal of Cleaner Production 270 (2020) 122040

Contents lists available at ScienceDirect

Journal of Cleaner Production

journal homepage: www.elsevier.com/locate/jclepro

Food waste biorefinery: Stability of an acidogenic fermentation system with carbon dioxide sequestration and electricity generation

Joana Ortigueira [a, b], Marta Pacheco [a], Maria Ascensão Trancoso [a], Pedro Farrancha [c], Jorge Correia [d], Carla Silva [b, **], Patrícia Moura [a, *]

[a] LNEG, Laboratório Nacional de Energia e Geologia, Unidade de Bioenergia e Biorrefinarias, Estrada do Paço do Lumiar, 1649-038, Lisboa, Portugal
[b] Instituto Dom Luiz, Faculdade de Ciências, Universidade de Lisboa, 1749-016, Lisboa, Portugal
[c] MSc Energy and Environment, Faculdade de Ciências, Universidade de Lisboa, 1749-016, Lisboa, Portugal
[d] Centro de Química Estrutural, Faculdade de Ciências, Universidade de Lisboa, 1749-016, Lisboa, Portugal

ARTICLE INFO

Article history:
Received 15 January 2020
Received in revised form
27 March 2020
Accepted 2 May 2020
Available online 4 June 2020

Handling editor. Panos Seferlis

Keywords:
Clostridium butyricum
Continuous stirred-tank reactor
Biohydrogen
Fuel cell
Organic acids
Nutrient recycling

ABSTRACT

The present study focused on the integration of the non-sterile conversion of food waste (FW) into hydrogen (H_2) through dark fermentation with the subsequent electricity generation in a proton-exchange membrane fuel cell (PEMFC), and the assessment of the global warming potential (GWP) of the process. The acidogenic conversion of FW performed in continuous operation for 16 days produced 45.6 ± 0.1 L H_2 at an average H_2 productivity of 6.1 ± 1.3 L L^{-1} d^{-1}. Butyric and acetic acid were simultaneously produced at average concentrations of 3.6 ± 0.5 and 1.6 ± 0.3 g L^{-1}, respectively. The carbon dioxide (CO_2) from biogas product was sequestered by reaction with sodium hydroxide and the resulting H_2-rich stream was fed to a PEMFC, producing 1.7 Wh L^{-1} H_2. The process scale-up was simulated based on the bench-scale conversion yields and was used to assess the GWP. Two of the developed scenarios, which considered the reuse of the fermentation sludge as nitrogen source in the acidogenic fermentation, diminished the GWP emissions by 63.8% and 64.3% when compared to the default condition. In the best-case scenario, an annual average of 0.18 t of CO_2 per t of FW separately collected was generated.

1. Introduction

Food waste (FW) is defined as food removed from the food production supply chain by voluntary or involuntary decision, without a defined purpose (European Parliament and Council, 2019). It is a direct result of human activity, being generated independently from social, cultural and economic variables (Lipinski et al., 2013). The analysis of FW generation patterns is hampered by the lack of data on national waste quantification, which does not allow identifying the critical loss or waste points in the food production supply line. According to available data, the results from quantitative studies vary greatly depending on selection factors such as: accounting for inedible food and liquid waste, destination of the waste, and distinction between waste/loss and avoidable/unavoidable (Corrado and Sala, 2018). The FW generation in EU-28 was estimated to range between 158 and 298 kg capita^{-1} y^{-1} (Stenmarck et al., 2016). According to current EU legislation, the waste disposed of in landfills must be reduced to maximum of 10% of the municipal waste generated by 2030, as leachates and gaseous emissions produced in the disposal facilities have severe harmful consequences for the environment (European Parliament and Council, 2018). In its place a more circular approach to the FW problem has been taken, in which there is a primary focus on decreasing FW generation by increased social awareness (i.e. reduction of avoidable waste) and recycling of unavoidably generated waste fractions as potential substrate for the production of energy, platform-chemicals, fertilisers, etc. (De Menna et al., 2018). Anaerobic conversion, particularly dark fermentation (DF), has been suggested as an appropriate bioconversion path for FW (Ortigueira et al., 2019a) as it is able to convert carbohydrates into hydrogen (H_2 or, when produced through the DF process, bioH_2),

* Corresponding author.
** Corresponding author.
E-mail addresses: joana.ortigueira@lneg.pt (J. Ortigueira), marta.pacheco@lneg.pt (M. Pacheco), maria.trancoso@lneg.pt (M.A. Trancoso), pedrofarrancha@gmail.com (P. Farrancha), jmcorreia@fc.ul.pt (J. Correia), camsilva@fc.ul.pt (C. Silva), patricia.moura@lneg.pt (P. Moura).

https://doi.org/10.1016/j.jclepro.2020.122040
0959-6526/

while achieving productivity values of more than 1 m^3 h^{-1} m^{-3} (Ren et al., 2011). Simultaneously, DF generates organic acids and sludge for which valorisation solutions such as the conversion to bioplastic precursors and the maturation to a nutrient-rich compost, respectively, are well-established (Bazyar Lakeh et al., 2019). Hydrogen is an energy carrier with a high energy content (120 MJ kg^{-1}), which can be efficiently converted into electricity through the use of proton-exchange membrane fuel cells (PEMFC). These cells consist of electrochemical devices typically composed by two electrodes separated by an ion selective electrolyte membrane (membrane-electrode assembly – MEA), which produce electricity through the conversion of H_2 and O_2 into water. The PEMFC can operate at relatively low temperatures (25–80 °C), tolerate small amounts of carbon dioxide (CO_2) in the fuel gas, and do not generate carbon or sulphur emissions (Gharehpetian et al., 2017). The conversion efficiency in regular PEMFC varies from 40 to 50% according to the operational temperature, and the H_2 pressure (Lin et al., 2007), reaching 80% yield when considering heat recovery (Kirubakaran et al., 2009). The ideal operational settings for these cells require impurity free fuel, i.e., the absence of carbon monoxide (CO), hydrogen sulphide (H_2S), ammonia (NH_3), nitrogen oxides (NO_x), among others, as these compounds can react with the components of the MEA. This will lead to poisoning of the electrode catalysts, thereby increasing the ionic resistance of the solid electrolyte and weakening the mass transfer due to alterations on the catalyst structure and wettability conditions, leading to an overall efficiency loss (Cheng et al., 2007). The listed impurities are generally consequence of the conventional H_2 production processes, particularly by hydrocarbon reforming, but they are uncommon in H_2-rich biogas produced through DF. Koroglu et al. (2019) investigated the conversion of biogas with 33–60% vol. of H_2 into electricity by a PEMFC, and correlated the presence of increasing amounts of CO_2 with a decrease in power density, which suggests that fermentation parameters should be optimised towards H_2 enrichment in the final biogas. The removal of CO_2 in the biogas before conversion through pressure swing adsorption or liquid adsorption produced positive results in the efficiency of the cell (Rahman et al., 2016).

There are several bench-scale biorefineries reported, focused on the conversion of FW into products of interest, such as plasticizers, lactic acid and animal feed (Kwan et al., 2015), surfactants (Pleissner et al., 2015), microalgae (Pleissner et al., 2013), biodiesel and bioethanol (Yang et al., 2014), lycopene and β-carotene (Kehili et al., 2016), phenolic acids and glycoalkaloids (Sánchez Maldonado et al., 2014) and H_2 (Huang et al., 2020). Most of these bench-scale biorefinery studies did not use real separately-collected FW, nor did they focus on FW conversion to electricity, organic acids and sludge. Furthermore, additional studies conducted by Falconer et al. (2020), Panigrahi et al. (2020), Rico et al. (2020) and Cheng et al. (2020) were mainly directed to the analysis of the FW pretreatment and fermentation stages, rather than quantification and analysis of the overall anaerobic production process. Therefore, the present study explored the use of separately-collected FW for the fermentative production of H_2-rich biogas to operate a PEMFC, of organic acids and sludge, the simulation of the process scale-up, and the assessment of the global warming potential (GWP) of the global integrated process through consequential analysis. The first part dealt with the integration of a continuous acidogenic fermentation system using catering industry waste (CIW) as feedstock and a PEMFC for electricity production, with the full characterisation of the process input and output streams (FW, sodium hydroxide (NaOH), organic acids, sludge, H_2 and CO_2). The continuous stirred-tank reactor (CSTR) operation was performed under non-sterile conditions and incorporated a substrate pretreatment step for microbial contamination control, the addition of *Clostridium butyricum*, a good microbial H_2 producer, as biocatalyst (Chen et al., 2005) and a CO_2 stripping stage for H_2 enrichment of the produced biogas. The H_2-enriched biogas was fed to a PEMFC and the cell performance was compared to its operation when supplied with commercial H_2 at 25 and 50 °C. The second part of the study sought to set-up the basis for an industrial process structured after a biorefinery model, where the FW conversion to multiple valuable products was modelled. For the stages of industrial mashing, microwave application, bioreactor operation and centrifugation, the bench-scale data were used alongside data from the literature concerning energy consumption values. The amount of 35000 t of FW collected annually by a Portuguese waste management operator that receives separately collected waste from restaurants, food markets, hotels and school canteens in the Lisbon metropolitan area was used for reference. Six scenarios were developed for the scaled-up biorefinery, which were compared with the direct energy consumptions and carbon dioxide equivalent (CO_{2eq}) emissions generated by the conventional FW treatment to produce electricity and compost by the waste management operator. The CO_{2eq} emissions of FW landfilling were also estimated.

2. Materials and methods

2.1. Food waste collection and conditioning

The FW used in this study was gathered from a local seafood restaurant located in the metropolitan Lisbon area, from Trafaria, Almada, on July 2018, and corresponded to the customary service food scraps (meat, fish, rice, vegetables, etc.), and leftovers from raw food preparation (vegetable peels, inedible parts of meat/fish removed during food preparation, etc.), collectively designated as CIW. This particular collection lasted approximately 8 h, which corresponded to a regular day of activity that includes one lunch and one dinner service. Materials that could not be mashed within laboratorial setting such as fish bones and hard seeds were removed from the mixture prior to biomass processing. The remaining material was mashed thoroughly, homogenised until a typical consistency was attained, and then stored at −20 °C until further use.

2.2. Bioreactor operation under non-sterile conditions

The bioreactor apparatus consisted in a 1.65 L bench-scale double jacketed glass reactor with a working volume of 0.5 L. The air-tight reactor was equipped with a pH sensor (405-DPAS–SC–K8S/250, Mettler Toledo, USA) and controller (MOD 7F, SGI, USA), and appropriate inlets/outlets for the following events: removal of gaseous product, removal of liquid fermentate, addition of fresh medium and carbon and energy source, pH control and addition of inoculum. The bioreactor setup is illustrated below (Fig. 1).

The operational settings were kept constant throughout the experiment. The pH control setpoint was defined as 5.5 ± 0.1 and controlled through the periodic addition of NaOH solution (2 mol L^{-1}). The temperature was maintained at 37 °C and stirring was adjusted to 300 rpm to avoid biomass settling inside the vessel.

The process start-up was performed as follows: 60.75 g of humid CIW (correspondent to approximately 10 g of total sugars and a final concentration of 20 g L^{-1} in the bioreactor) were subjected to microwave (MW) pretreatment, as described elsewhere (Ortigueira et al., 2019a). This mixture was suspended in minimum mineral medium as already published (MMM) (per L of phosphate buffer 100 mM: 12 g ammonium chloride, 3.28 mg ferrous sulphate heptahydrate, 0.56 g cysteine hydrochloride monohydrate), up to a total volume of 500 mL and degassed with N_2 for 1 h (Ortigueira

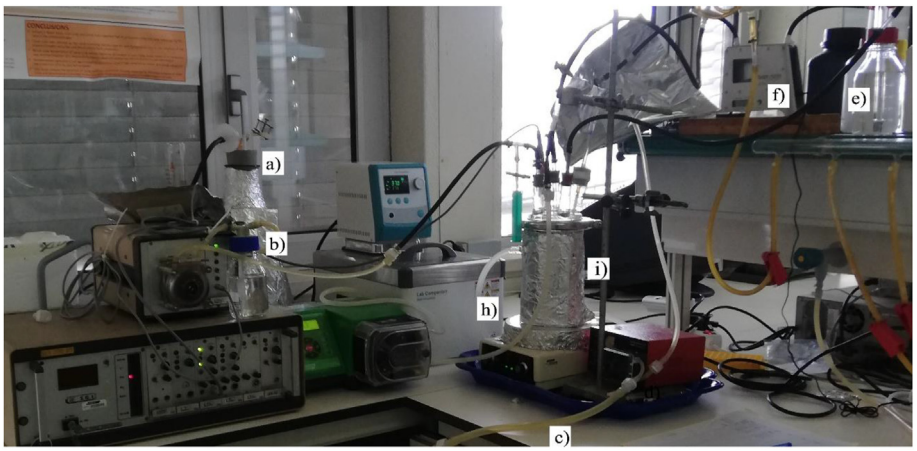

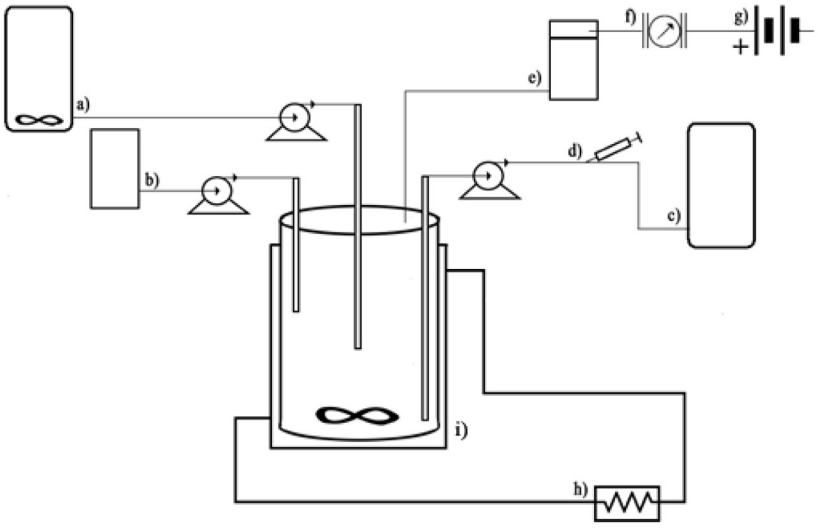

Fig. 1. Schematic representation of the continuous stirred-tank reactor (CSTR): a) catering industry waste (CIW) + minimum mineral medium (MMM) feed; b) NaOH solution for pH control; c) effluent; d) sampling port; e) NaOH scrubber for CO_2 sequestration; f) Flowmeter; g) proton-exchange membrane fuel cell (PEMFC); h) Water bath for temperature control; i) double jacketed glass bioreactor.

et al., 2019a). *Clostridium butyricum* DSM 10702, from the German Collection of Microorganisms and Cell Cultures (DSMZ, Braunschweig, Germany) was used to inoculate the non-sterile mixture at a volumetric concentration of 5%. This inoculum was pre-cultured in Reinforced Clostridial Medium (RCM) (Difco laboratories, France) for 16 h prior to the fermentation start-up. After 24 h of operation, the fermentation mode was shifted from batch to CSTR.

The CSTR operation was performed as follows: 516.4 g of humid biomass was subjected to MW pretreatment as described previously (Ortigueira et al., 2019a). The resulting material was suspended in MMM medium up to a total volume of 5 L, resulting in a final concentration of total sugars of 17 g L^{-1}. The referred solution, hereby defined as feed solution, was used to fill the bioreactor communicating vessel, degassed with N_2 and then added to the reactor through the appropriate inlet at a flow of 67.8 mL h^{-1}. The hydraulic flow was equivalent to a hydraulic retention time (HRT) of 7.4 h and the addition of 1.15 g $_{\text{total sugars}}$ h^{-1}. The fermentate was removed from the bioreactor at the same flow, to avoid culture volume variation. The liquid samples were collected through the appropriate outlet every 24 h for characterisation and quantification of total sugars and soluble metabolites by high performance liquid chromatography (HPLC). The gaseous product generated inside the bioreactor, mainly composed by H_2 and CO_2, was continuously conducted through a scrubber with NaOH solution (2 mol L^{-1}) for CO_2 sequestration. The resulting gas was conducted through a flowmeter (μflow, Bioprocess Control, Sweden) for data collection at standard pressure and temperature conditions (STP). The outlet of the apparatus was connected to appropriate air-tight gas collecting bags (Flexfoil® sample bags, SKC, United Kingdom) for the final collection of the H_2-enriched biogas.

2.3. Fuel cell on-set and characterisation

A bench-scale PEMFC (Parker TekStak Fuel Cell, Parker Hannifin, USA) was integrated with the CSTR bioreactor. The fuel cell was composed by graphite gas distribution end plates, a Nafion electrolyte membrane (10.89 cm^2 of membrane area) covered with a porous carbon layer with dispersed platinum (4 mg cm^{-2}) and platinum-ruthenium (4 mg cm^{-2}) catalysts on the cathodic and anodic sides of the cell, respectively. Prior to use, the PEMFC was assembled according to the instructions provided alongside the device and inserted into the experimental setup depicted in Fig. 2.

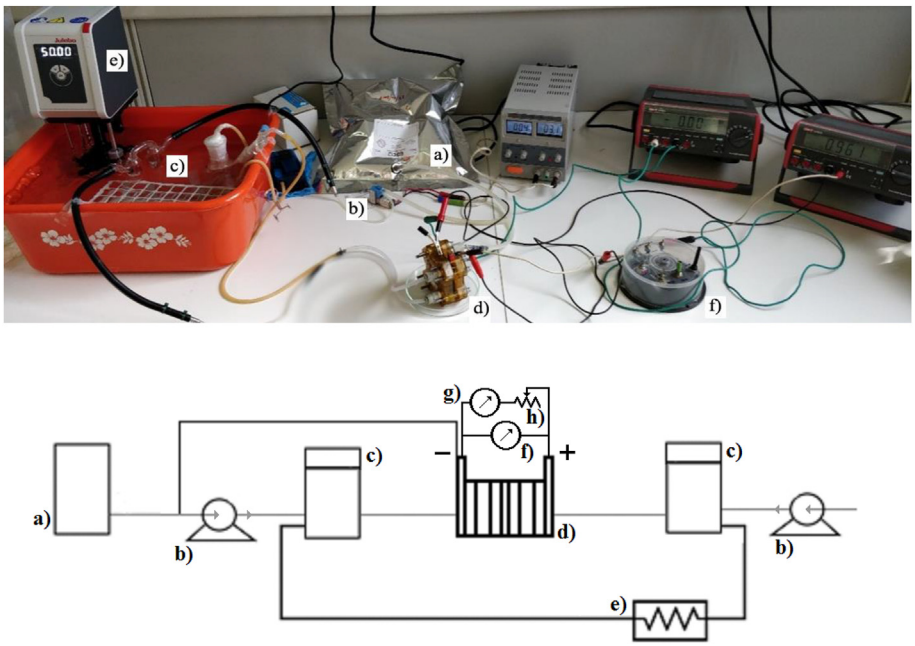

Fig. 2. Schematic representation of the fuel-cell apparatus: a) bioH_2 sample; b) gas pump; c) gas washing bottles (bioH_2; air); d) fuel cell; e) water bath for temperature control; f) voltmeter; g) ammeter; h) potentiometer.

The PEMFC was connected in series with an ammeter and a potentiometer and in parallel with a voltmeter (Fig. 2). The biogas sampling bag (a) was attached to a gas pump for flow regulation (b) and forced through a water bath where the gas was humidified and heated to an operational temperature (c) prior to insertion on the anodic side of the cell. Atmospheric air was subjected to the same conditions in order to feed the cathodic side of the cell. The PEMFC was tested with commercial H_2 (approximately 100% H_2 purity) and bioH_2 under two operational temperatures (25 and 50 °C). The content of the later feed gas varied according to the fermentation performance, and was composed mainly of H_2 and vestigial traces of N_2. The bioH_2 was kept humid and added sequentially for improvement and characterisation of the fuel cell performance, respectively. Polarisation and power density curves were drawn with the obtained data, by modulating the load resistance with the potentiometer, in order to attain the relation between bioH_2 flow ($\dot{m}_{H2}$) and power (P). Power is measured by voltage (V) and current (I),

$$P[W] = VI \tag{1}$$

the H_2 flow was obtained from Larminie and Lowry (2012).

$$\dot{m}_{H2}\left[\frac{mL}{h}\right] = \dot{n}_{h2} * \frac{RT}{P}\left[\frac{m^3}{mol}\right] * 10^6\left[\frac{mL}{m^3}\right] * 3,600\left[\frac{s}{h}\right] \tag{2}$$

where $\dot{n}_{h2}$ is the molar mass flow (mol s^{-1})

$$\dot{n}_{h2} = \frac{I}{2F}\left[\frac{mol}{s}\right] \tag{3}$$

F is the Faraday's constant (96485.3 C mol^{-1}), I is the current (A), R is the universal gas constant (8.314 J mol^{-1} K^{-1}), T is the trial temperature (K) and P the ambient pressure (100 kPa). The efficiency η of the PEMFC can be obtained through equation (4):

$$\eta = \frac{P}{HHV * \dot{n}_{h2}} \tag{4}$$

where HHV represents the higher heating value of H_2, assuming the water is removed from the system in liquid form (−285.83 kJ mol^{-1}). The target ratio of $P/\dot{m}_{H2}$ can be derived by using the equations above

$$\frac{P}{\dot{m}_{H2}}\left(W/L/h\right) = \frac{\eta * HHV}{\frac{RT}{P} * 10^3 * 3600} \tag{5}$$

For STP and η = 0.5, this procedure retrieves 1.96. Rahman et al. (2016) also considered a fuel utilisation coefficient, μf, of 0.95, reducing the $\frac{P}{\dot{m}_{H2}}\left(W/L/h\right)$ to 1.86. This value was validated through experimentation. A total of ten assays were performed with bioH_2 and commercial H_2 at the temperatures of 25 and 50 °C.

2.4. Analytical methods

2.4.1. Proximal characterisation of the food waste

The CIW samples were analysed according to standard methods (Horwitz and Latimer, 2005) for total sugars and fat, crude protein, moisture and ash. Total sugars were determined after acidic pre-treatment with H_2SO_4 (720 g kg^{-1}) according to standard methods (Horwitz and Latimer, 2005) followed by quantification through an

Table 1
Proximal composition of the processed catering industry waste (CIW) used in the fermentation experiments, by dry weight (d.w.).

Component	% d.w.
Total sugars	62.1 ± 0.1
Crude protein	10.4 ± 0.2
Total fat	26.3 ± 2.2
Ash	1.2 ± 0.1

adapted anthrone method as already published (Ortigueira et al., 2019a). The results are displayed in Table 1.

2.4.2. Characterisation of the fermentation products

The samples of the collection bags were analysed in a gas chromatographer (GC) (Varian 430-GC, Agilent technologies, USA) equipped with a thermal conductivity detector (TCD). The H_2 and CO_2 quantification was performed using a fused silica column (Select Permanent Gases/CO_2-Molsieve 5A/Borabound Q Tandem #CP 7430). The injector and oven were operated at 80 and 70 °C, respectively and the detector at 120 °C. Argon was the carrier gas at a rate of 32.4 mL min^{-1}. The TCD was kept at 220 °C.

The liquid samples were purged of solid residues by centrifugation (15000 rpm) and vestigial oil/fat was subsequently removed by hexane extraction (Ortigueira et al., 2019a). The resulting aqueous phase was filtered (0.2 μm) and analysed in a HPLC system (LaChrom, Merck, Germany) equipped with an Aminex HPX-87H column (Bio-Rad Laboratories, USA) and a refraction index (RI) detector (LaChrom L-7490, Merck, Germany). The temperature of the column and the RI detector were kept constant at 50 °C and 45 °C, respectively, and samples were eluted using H_2SO_4 5 mM (flow rate = 0.5 mL min^{-1}). Solutions of carboxylic acids were used as external standards. The nitrogen and total sugar content of the solid fraction (sludge) were quantified according to standard methods (Horwitz and Latimer, 2005) and a modified anthrone method as published elsewhere (Ortigueira et al., 2019a). Elemental characterisation of the substrate feed and fermentation sludge were performed according to standard methods (ISO, 18122:2015, ISO 16948:2015, EN 15289:2011, ionic chromatography) as already published (Ortigueira et al., 2019b). The characterisation results are summarised in Table 2.

2.4.3. Growth and fermentation parameters

The lag phase of the fermentation assay corresponded to the time required for the detection of biogas production. The total H_2 production was calculated as being the sum of the volume of H_2 collected in the collection bags during the course of the experiment, herein expressed as cumulative H_2 production, as well as the volume of H_2 that remained inside the bioreactor headspace at the end of the fermentation assay. The molar quantification of H_2 and CO_2 was calculated through the Peng-Robinson equation (Ortigueira et al., 2015). Hydrogen productivity was estimated from the graphical representation of the cumulative H_2 production (L L^{-1}) *versus* time (hours), as the slope of the production tendency obtained for each 24-h period. The H_2 molar yield was defined as the ratio between the total amount of H_2 (mol) produced throughout the experiment and the total sugars consumed (mol), expressed as glucose equivalents. The volumetric H_2 yield was defined as being the ratio between the total H_2 volume (L) produced and the mass of CIW (kg of volatile solids) supplied to the culture medium. Both yields were calculated in 24-h intervals, and gas volumes were determined at STP.

Table 2
Elemental characterisation of the feed supplied to the continuous stirred-tank reactor (CSTR) and the produced sludge, by dry weight (% d.w.).

Elements	Feed (CIW + MMM)[a]	Sludge[a]
Carbon	22.7	8.4
Hydrogen	5.5	3.6
Nitrogen	7.1	6.6
Chloride	3.2	0.6
Sulphur	0.065	0.05

[a] % d.w.; CIW, catering industry waste; MMM, minimum mineral medium.

2.5. Process scale-up

The integrated FW fermentation and PEMFC operation considered the following process stages: mashing, microwave pretreatment, acidogenic fermentation, gas stripping, centrifugation, electricity production from obtained bioH_2, and recirculation of fermentation sludge. The system to scale-up is depicted in Fig. 3.

The scale-up was performed based on the amount of organic waste separately collected by one waste management system, which was operating in the municipality of Lisbon in the year of 2018 (Valorsul, 2018). Considering that the waste was collected mainly in food markets and canteens, green residues were considered negligible, and the overall collection was equalled to FW and assumed to be the available substrate for acidogenic conversion. The amount of separately collected organic waste in 365 days of operation, which totalised 35000 t, was defined as the functional unit (FU). This value is equivalent to approximately 4 t per hour, which corresponds to a total volumetric flow of feed (i.e., biomass and fermentative medium) of 930.6 m^3 h^{-1}. The ratio between volumetric feed flow and the reactor volume was kept from the bench-scale to the scale-up (0.14). For this production to be viable, two bioreactors would be required, equalling an overall volume of 200 m^3 (useful volume of 143 m^3, assuming a reactor occupation of approximately 70%). All unitary operations were based on the value of feed indicated, assuming bench-scale yields were kept constant. The same factor was applied to the relation between the power and H_2 flow (Fig. 8, section 3.2.) which, according to lab data, indicates that the conversion of 1 L of H_2 will produce 1.7 Wh of electricity. The industrial PEMFC dimensions were obtained by knowing the maximum industrial H_2 flow with $\eta = 50\%$, for maximum power. Accordingly, for the 72.7 m^3 H_2 h^{-1} production predicted from the scale-up, the stack maximum power should be 123.5 kW. An inverter was introduced into the system after the PEMFC in order to convert direct current (DC current), which was obtained through the fuel cell operation, into alternate current (AC current). The efficiency of the inverter was defined as 94% (Nishikawa et al., 2008). The energy consumption values used for scale-up calculations were based on data from prior literature and were registered in Table 3.

2.6. Reference system for FW valorisation

The "Valorsul" company is responsible for the urban solid wastes (USW) collection and treatment in 19 municipalities from the Lisbon and West regions of Portugal, dealing with circa 20% of the USW generated in Portugal (1.3 kg of urban waste $capita^{-1}$ d^{-1} for the year of 2017). The waste treatment system is composed by, among others, an organic anaerobic digestion unit (OADU) with an installed capacity of 28 t h^{-1}, i.e., capable of processing 60000 t of waste into biogas per year (Valorsul, 2018). This particular stage consumes between 4 and 6 GWh y^{-1} with a total yearly production of 8–12 GWh of electricity, through biogas burning, and 9800–14700 t of compost. The biomass used in the process is separately collected from restaurants, food markets, hotels and school canteens. The OADU unit is, by definition, a biorefinery as shown in a simplified scheme in Fig. 4, involving various stages of pretreatment, drying, weighting, dehydration, etc. This installation was compared to the integrated system proposed in this study, based on the bench-scale results. The nitrogen content of the "Valorsul" compost was obtained from commercial information available online (2.3% w/w).

Reported only in support of the discussion is the case in which FW was not valorised by enabling its complete decomposition without human intervention. In order to calculate the input of biogenic CO_2 for the conversion process, the carbon content of 22.7 $\%_{d.w.}$ determined in the elemental characterisation of the feed

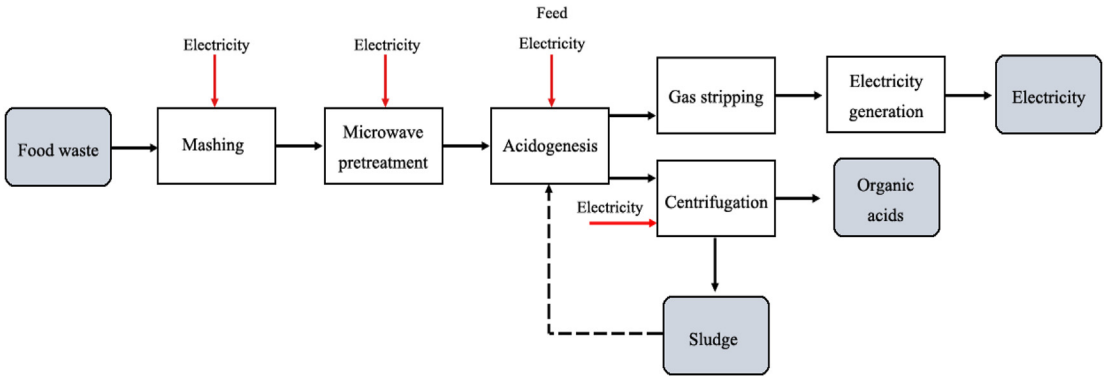

Fig. 3. Flowchart of the process stages, substrate and electricity inputs, and product outputs considered in the integrated food waste (FW) fermentation and proton-exchange membrane fuel cell (PEMFC) operation.

Table 3
Energy consumption of the industrial equipment considered for the scaled-up model of the biorefinery.

Industrial equipment	Energy consumption	Reference
Industrial masher	1.1 kWh t^{-1} biomass	De Marco et al. (2018)
Microwave	168 kWh t^{-1} biomass	Olatunde et al. (2017)
Reactor	5.4 kWh m^{-3} feed	Collet et al. (2011)
Centrifuge	5.5 kWh t^{-1} biomass	Soda et al. (2010)

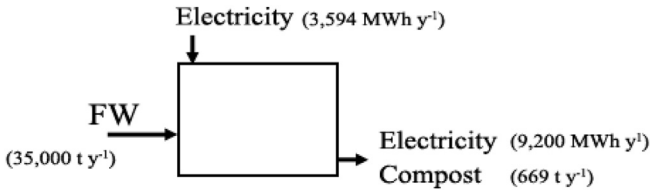

Fig. 4. Schematic representation of the organic anaerobic digestion unit (OADU) from the "Valorsul" valorisation unit (Valorsul, 2018) that was considered as reference for the biological treatment of food waste (FW).

(Table 2, section 2.4.2.), was applied to the FU. According to this calculation, a total of 2018 t of carbon were introduced into the system for conversion. Without valorisation, the entirety of the carbon present in the biomass would be converted into CO_2, leading to a maximum yield of 0.21 t of CO_2 per t of waste biomass or 7350 t of CO_2 y^{-1}. This was considered the most unfavourable condition, in which no product nor energy recovery was derived from the process, and the entirety of carbon content would be lost as biogenic CO_2 emission.

2.7. Design of scenarios and system comparison

The production data obtained in the experimental stage were utilised as a basis for the projection of a possible scaled-up production, and compared to the data obtained from the biological conversion system used as reference (Fig. 4). To make the comparison in terms of direct energy consumption and global warming potential ($GWP_{100\ years}$), a consequential approach was followed, i.e, marginal supply and demand on affected markets was taken into consideration and allocation was avoided by system expansion. In practice, the same input of FW was considered and its associated outputs such as electricity (MWh y^{-1}) and compost (t y^{-1}). Excess electricity, compost and additional byproducts were considered as credits (−) or burdens (+) in the alternative systems. The CO_{2eq} values for the consumables of the processes were taken from Ecoinvent 3 and other sources of the literature in order to obtain a range of emissions instead of a unique quantity (Table 4). Several cases of study were considered for analysis: FW without valorisation, FW valorisation through anaerobic digestion (reference) and the following scenarios with basis on the FW acidogenic biorefinery:

- **Scenario 1** or default scenario (Sc#1). The FW is processed into H_2, organic acids (butyrate, acetate, lactate and formate) and sludge. Microwave pretreatment is performed in the waste treatment facility. Biogenic CO_2 sequestration takes place during the gas stripping stage with associated production of sodium hydrogen carbonate.
- **Scenario 2** (Sc#2). The FW is processed into H_2, organic acids (butyrate, acetate, lactate and formate) and sludge. Microwave pretreatment is performed at household level. Biogenic CO_2 sequestration takes place during the gas stripping stage with associated production of sodium hydrogen carbonate.
- **Scenario 3** (Sc#3). The FW is processed into H_2 and organic acids (butyrate, acetate, lactate and formate). The fermentation sludge is recirculated into the system as nitrogen source. Microwave pretreatment is performed at household level. Biogenic CO_2 sequestration takes place during the gas stripping stage with associated production of sodium hydrogen carbonate.
- **Scenario 4** (Sc#4). The FW is processed into electricity and organic acids (butyrate, acetate, lactate and formate). The fermentation sludge is recirculated into the system as nitrogen source. Microwave pretreatment is performed at household level. Biogenic CO_2 sequestration takes place during the gas stripping stage with associated production of sodium hydrogen carbonate.
- **Scenario 5** (Sc#5). The FW is processed into H_2 and organic acids (butyrate, acetate, lactate and formate). The fermentation sludge is recirculated into the system as nitrogen source. Microwave pretreatment is performed at household level. Biogenic CO_2 is not sequestered.
- **Scenario 6** (Sc#6). The FW is processed into electricity and organic acids (butyrate, acetate, lactate and formate). The fermentation sludge is recirculated into the system as nitrogen source. Microwave pretreatment is performed at household level. Biogenic CO_2 is not sequestered.

The reference and alternative scenarios are depicted in Fig. 5, including input and output information.

To account for uncertainty, calculations were performed based on the average GWP values prior to a range evaluation. The electricity carbon intensity is highly dependent on the country and year

Table 4
Global warming potential (GWP) of the main consumables and products identified in the different processes.

Item	GWP range (kg CO_{2eq} kg^{-1})	Average GWP (kg CO_{2eq} kg^{-1})	Reference
Acetic acid	1.11–1.57	1.34 ± 0.23	(Ecoinvent database, 2016)
Ammonium chloride	1.37–3.29	2.33 ± 0.96	(Ecoinvent database, 2016)
Butyric acid	3.31–3.46	3.38 ± 0.07	Own calculations
Disodium phosphate	1.58	1.58 ± 0.00	Hervy et al. (2015)
Electricity	296–524	377.5 ± 81.5	European Environmental Agency (2019)
Fertiliser (N)	4.62–5.88	5.25 ± 0.63	(Ecoinvent database, 2016)
Formic acid	1.43–2.91	2.17 ± 0.74	(European Commission Joint Research Centre et al., 2014) Ecoinvent database (2016)
Commercial hydrogen	0.97–12.9	6.94 ± 5.97	Water Technology (2012)
Iron sulphate	0.17–0.23	0.20 ± 0.03	(Ecoinvent database, 2016)
Lactic acid	3.97–4.95	4.46 ± 0.49	(Ecoinvent database, 2016)
Monosodium phosphate	2.32–2.96	2.64 ± 0.32	(Ecoinvent database, 2016)
Sodium hydrogen carbonate	0.24–1.17	0.71 ± 0.47	(Ecoinvent database, 2016) Water Technology (2012)
Sodium hydroxide	0.41–1.21	0.81 ± 0.40	(Ecoinvent database, 2016) Cetinkaya et al. (2012)

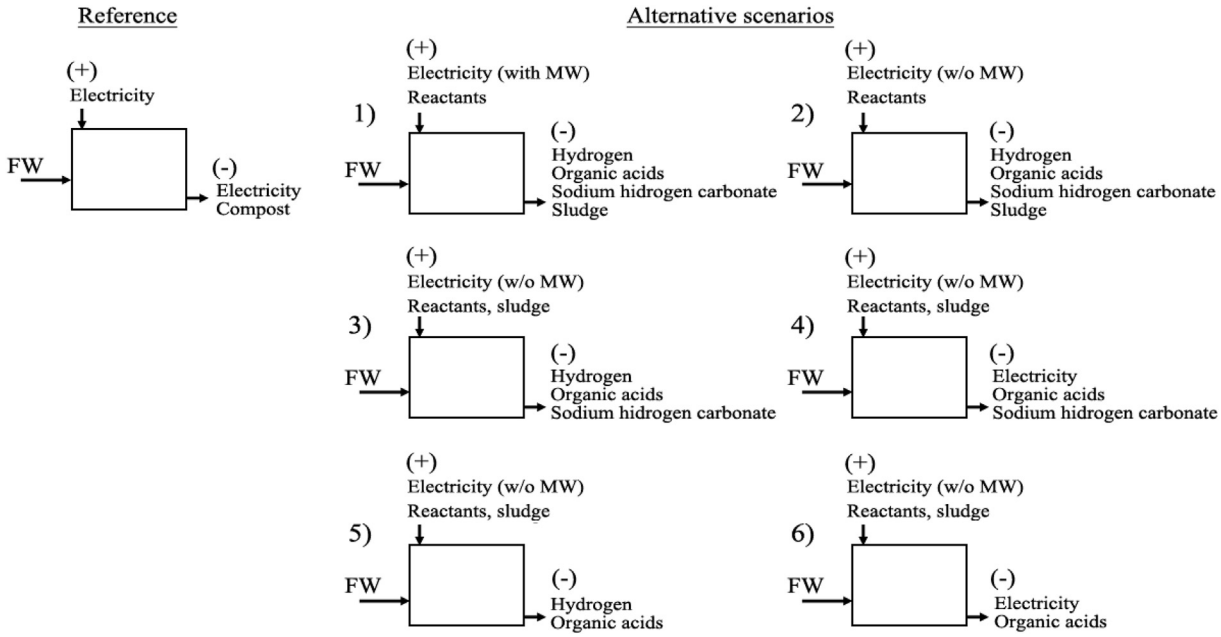

Fig. 5. Schematic representation of the reference and alternative scaled-up valorisation systems and market influences considered for equivalency (credits (−) or burdens (+) for CO_{2eq}).

of electricity production. To capture this effect on the calculations, results are depicted as a function of the electricity carbon intensity (European Environmental Agency, 2019). The products of the fermentation process were considered in the scenarios if they were produced in significant concentrations (>1 g L^{-1} in the fermentate) and if they were of broad commercial importance, particularly for the chemical and pharmaceutical industry. The value of GWP for butyric acid production was not available in literature nor in correspondent databases. Therefore, it was estimated from the biological process of the present study through an economic allocation based on Sc#1 and Sc#2. Table 5 depicts the current commercial prices for product and byproducts of the fermentative process, and GWP were calculated according to the economic allocation procedure.

The value for GWP of the L-cysteine hydrochloride was not available in the literature and could not be estimated due to lack of production data. Therefore, it was not considered. The compost and sludge obtained from the reference and acidogenic systems, respectively, were compared to fertiliser in accordance with their nitrogen content (see section 2.6 and Table 2 in section 2.4.2.). The range of GWP for electricity was imposed after analysis of the CO_2 intensity data for the year of 2016 (European Environmental Agency, 2019). The current electricity mix (CEM) corresponded to the best possible scenario, in which a higher fraction of the electricity mix was from renewable energy sources (2016 data). A low-renewable electricity mix (LREM) was also considered, corresponding to the worst-case scenario in which a larger fraction of the mix would come from non-renewable energy sources (1990 data).

3. Results and discussion

3.1. Stability of continuous bioH_2 production from pretreated CIW, with addition of C. butyricum, in a bench-scale setting

The continuous non-sterile H_2 production from highly contaminated substrates, such as FW, is influenced greatly by the diversity and activity of the substrate native microorganisms that

Table 5
Input data for economic allocation and corresponding global warming potential (GWP) per considered product for scenarios Sc#1 and Sc#2.

Fermentation products	Price (€ kg^{-1})[a]	Proceeds (M€ y^{-1})	GWP based on Sc#1 1 (kg CO_{2eq} kg^{-1})	GWP based on Sc#2 (kg CO_{2eq} kg^{-1})
Hydrogen	12.5	0.7	0.7	0.7
Acetic acid	28.7	16.7	1.6	1.7
Butyric acid	58.9	79.0	3.3	3.5
Lactic acid	62.5	45.6	3.5	3.7
Formic acid	24.5	9.6	1.4	1.4
Sludge	5.3	52.1	0.3	0.3
Sodium hydrogen carbonate	53.9	290.7	3.0	3.2

[a] prices referenced from ChemicalBook (2016).

enter into the bioconversion system. The coexistence of different metabolic pathways may divert the conversion of sugars to undesired final products and cause the decline of H_2 production. Promising results were obtained with the application of MW to CIW as a means of reducing the initial contamination of the substrate before starting the batch fermentation for H_2 production (Ortigueira et al., 2019a). However, it is important to accurately assess the mid-term impact of such a MW pretreatment on the stability and performance of non-sterile bioaugmented fermentations operated under continuous mode. With this purpose, a CSTR bioreactor was operated for a total of 16 days for the non-sterile acidogenic conversion of MW-pretreated CIW. The profiles of the daily and cumulative biogas and H_2 production in the bioreactor are illustrated in Fig. 6.

The feed and HRT imposed upon the system were based on the consumption rate of total sugars by *C. butyricum* which was determined in a previous study (Ortigueira et al., 2019a). Accordingly, the feed suspension was introduced into the reactor at a flow rate of 1.15 g $_{total\ sugars}$ h^{-1} under a constant HRT of 7.4 h. This value is consistent with the information reported by Sivagurunathan et al. (2016), in which low values of HRT are conducive to more efficient acidogenic fermentations. Theoretically, a low HRT maintains the acidogenic microorganisms in exponential growth and minimises the proliferation of H_2-consuming microorganisms within the mixed culture. The results obtained from day 1–5 (Fig. 6) show that the bacterial community was still adapting to the new hydraulic regimen, marked by the large increment in the volumetric biogas production from 4.0 up to 8.7 L L^{-1} d^{-1}. At this point, the concentration of H_2 in the produced biogas achieved 98.2 ± 1.0% vol. after CO_2 stripping. Subsequently, the H_2 production remained consistent throughout the course of the experiment, steadying at an average volumetric production of 6.1 ± 1.3 L H_2 L^{-1} d^{-1} and a H_2 concentration in the output biogas of 95.8 ± 1.0% vol. (Table 6). The exception to the tendency displayed occurred in day 6 and 13, wherein problems with the stirring of the feed stream were experienced; these were caused by an infrequent accumulation of solid particulates. These results are dissimilar to those registered by Kanchanasuta et al. (2017). The authors found that when the *C. butyricum* strain TISTR 1032 was used as biocatalyst in non-sterile fed-batch FW fermentations, the registered total H_2 production was higher during the first substrate feed (24 h of operation). During the second feed, a reduction of approximately 70% in total H_2 production was observed. In the present study, the H_2 productivity and production yield, while variable, were consistent throughout the experiment. With exception of day 6 and 13 of operation (Fig. 6), the system was constantly able to deliver, from day 5 to day 16 of process time, a highly H_2-enriched biogas in the range of 4.9–8.7 L L^{-1} d^{-1}. This result supports the assumption stating that the MW pretreatment, while not able to eliminate all the CIW native microorganisms, is able to partially control the activity of native microorganisms and maintain the H_2 production by *C. butyricum* within the microbial consortium. No methane (CH_4) was detected in the biogas produced, i.e., the methanogenic activity was supressed or inexpressive due either to the application of the MW pretreatment or the low HRT imposed upon the system (Alexandropoulou et al., 2018).

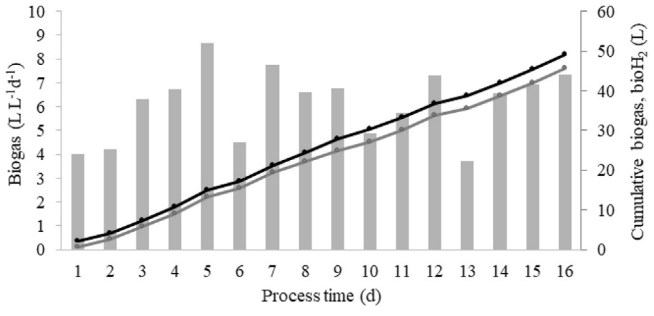

Fig. 6. Daily biogas production (columns) and time-course of accumulated biogas and H_2 (biogas – ●; H_2 – ●) in a continuous stirred-tank reactor (CSTR) fed with microwave (MW) pretreated catering industry waste (CIW), under non-sterile conditions and with addition of *C. butyricum* as biocatalyst.

Sugar consumption under CSTR operation increased visibly throughout the fermentation cycles, up to a maximum of 94.1 ± 2.6% (w/w) by day 16 (Table 6). This was likely associated with the adaptation of the microbial consortium to the substrate and the accumulation of enzymatic compounds in the fermentation medium, enabling the degradation of polymeric carbohydrates to a greater extend compared to the initial fermentation time. This may also be attributed to the persistence of native microorganisms of the CIW-feed, which may play a role in cross-feeding or exhibiting enzymatic traits complementarity to *C. butyricum*. An average H_2 yield of 74.9 ± 15.8 L H_2 kg^{-1}_{VS} or 110.7 ± 22.5 L H_2 $kg^{-1}_{total\ sugars}$ was obtained during the steady-state phase of the CSTR operation, between day 3 and day 16 (Table 6). These values represent a clear decrease when compared to the yields obtained previously under batch operation (Ortigueira et al., 2019a). They point to the presence of microbial populations that deviate carbohydrates to non-H_2 producing metabolic pathways. To counteract this effect, several authors suggested an increase of the fermentation temperature such as, for example, Youn and Shin (2005) who obtained H_2 yields in the range of 125 L H_2 kg^{-1} $_{VS}$ under thermophilic conditions. In the present study this option was disregarded, as it would be associated with higher energetic costs. A second option was suggested within the same study, which consisted of using a microbial consortium adapted to the substrate and imposing a low HRT or a high operational temperature as selective pressure to supress the activity of undesirable microorganisms. Qin et al. (2019), De Gioannis et al. (2017) and Algapani et al. (2019) obtained H_2 yields of 50.0, 56.5 and 135.0 L kg^{-1} $_{VS}$, respectively, with the latter strategy, the last value being considerably higher than that obtained in the present study. However, the yield per unit of substrate biomass is highly dependent on its chemical composition and it is

Table 6
Average production parameters obtained during the 16 days of operation of the continuous stirred-tank reactor (CSTR) for the conversion of catering industry waste (CIW).

Total sugars consumption (%)	Total H_2 production (L)	Average H_2 productivity (L L^{-1} h^{-1})	Average H_2 in the biogas (% vol)	H_2 yield (L kg^{-1}_{VS})	Butyrate-to-acetate ratio
94.1 ± 2.6	45.6 ± 0.1	6.1 ± 1.3	95.8 ± 1.0	74.9 ± 15.8	1.9 ± 0.4

likely that an increase in carbohydrate concentration may impact significantly the overall production yield. Conversely, the H_2 productivity registered in the present study reached 6.1 ± 1.3 L L^{-1} d^{-1}, which is considerably higher than 3 L L^{-1} d^{-1} obtained by Algapani et al. (2019).

Previous studies on the fermentation of carbohydrate-containing biomass by *C. butyricum* identified butyric and acetic acid as the main byproducts of sugar conversion (Ortigueira et al., 2019a). The concentration of organic acids throughout the operation of the CSTR averaged 5.2 ± 0.8 g L^{-1}, being composed mainly by acetate and butyrate, which corresponded to approximately 19 and 44% of the total acids produced, respectively. The average butyrate-to-acetate ratio was 1.9 ± 0.4 (Table 6), indicating the slight shift towards butyrate production, which is generally associated with high H_2 partial pressure (Ortigueira et al., 2019a). Lactate was also produced , particularly after day 5 (Fig. 7). Unlike acetate and butyrate, lactate is not linked with H_2 production, and was associated with the presence of microbial contaminants in the substrate (Harzevili and Hiligsmann, 2017). The MW pretreatment was originally introduced in order to control the substrate contamination, particularly by lactic acid bacteria, which caused the carbon source to deviate into undesirable metabolic pathways. However, this effect became less apparent after the first 5 days of fermentation, resulting in a highly variable lactic acid concentration (0.4–3.2 g L^{-1}) up until the end of the process time. These results led to the conclusion that lactic acid bacteria persisted in the substrate after pretreatment and in the bioreactor during fermentation.

In summary, the results of H_2 production showed a stable performance of the CSTR throughout the process runtime, although some metabolic activity directed to the production of lactic acid was noted.

3.2. Electricity generation from bioH_2 in a bench-scale setting

The biogas produced during the operation of the CSTR was composed of CO_2 and H_2, most likely in a humidified state due to evaporation of the culture medium. The CO_2 sequestering stage caused all the produced CO_2 to react with a supplied solution of NaOH. This process was associated with the production of sodium hydrogen carbonate and resulted in a H_2-enriched biogas sample

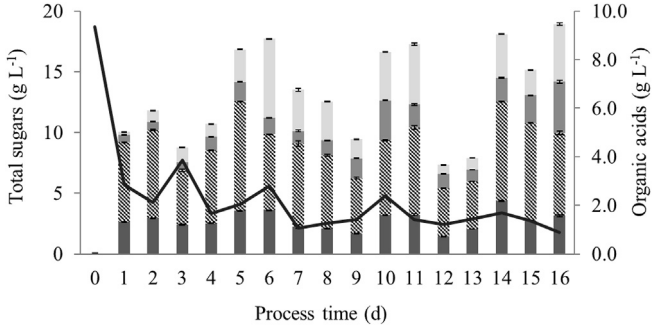

Fig. 7. Time-course of total sugars consumption (black line) and organic acids production (acetate – ■; butyrate –; formate – ■; lactate – ■) in a continuous stirred-tank reactor (CSTR) fed with microwave (MW) pretreated catering industry waste (CIW), under non-sterile conditions and with the addition of *C. butyricum* as biocatalyst.

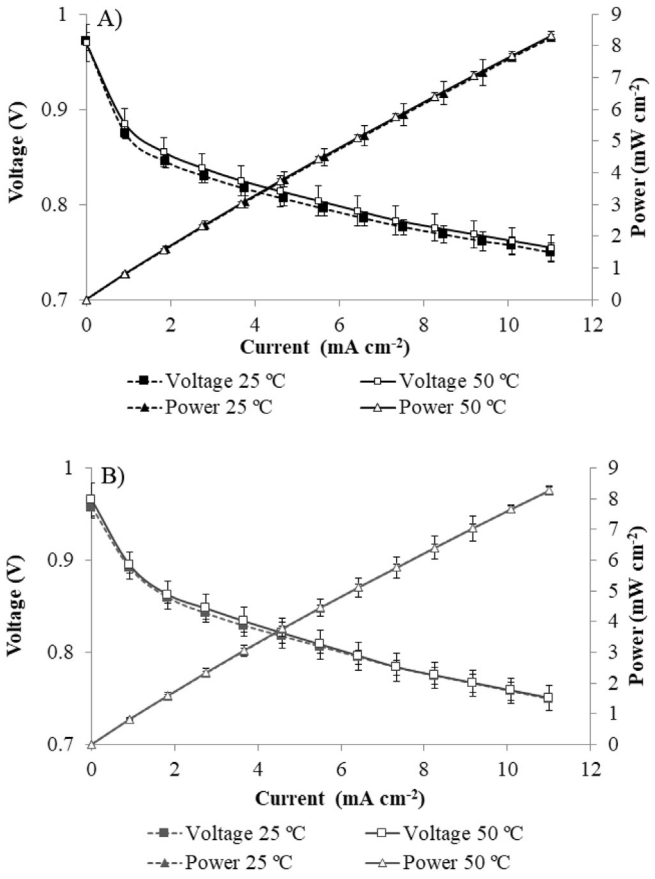

Fig. 8. Polarisation and power density curves for the lab-scale fuel cell operated with: A) bioH_2 produced during the operation of the continuous stirred-tank reactor (CSTR); B) commercial H_2.

(averaging 95.8% vol. purity). This sample was fed to a PEMFC at two operational temperatures, 25 and 50 °C. For comparison purposes, the same experimental setup was undertaken with commercial H_2 (>99% purity) in order to ascertain if biogas characteristics would impact the PEMFC performance. The experimental polarisation and efficiency curves are depicted in Figs. 8 and 9 for bioH_2 and commercial H_2.

Fig. 8A compared the information obtained through the operation of the PEMFC with the bioH_2 at the two operational temperatures. Values of voltage measured for both systems registered a slight increase with the increasing temperature but the variation was not considered statistically significant. In fact, the same effect was noted upon analysis of the power measurements for both temperatures, which once again proved to be nearly indistinguishable. This result seems to contradict known literature which states that temperature increase should impact positively on the PEMFC performance (Lin et al., 2007). This deviation in behaviour might be indicative of further increase in temperature (80–100 °C) being required or is a result of the operational setting. The stage for biogas/air temperature control should have, theoretically, increased the overall temperature of the gas and of the PEMFC. However, the PEMFC itself as well as connecting pathways were not subjected to

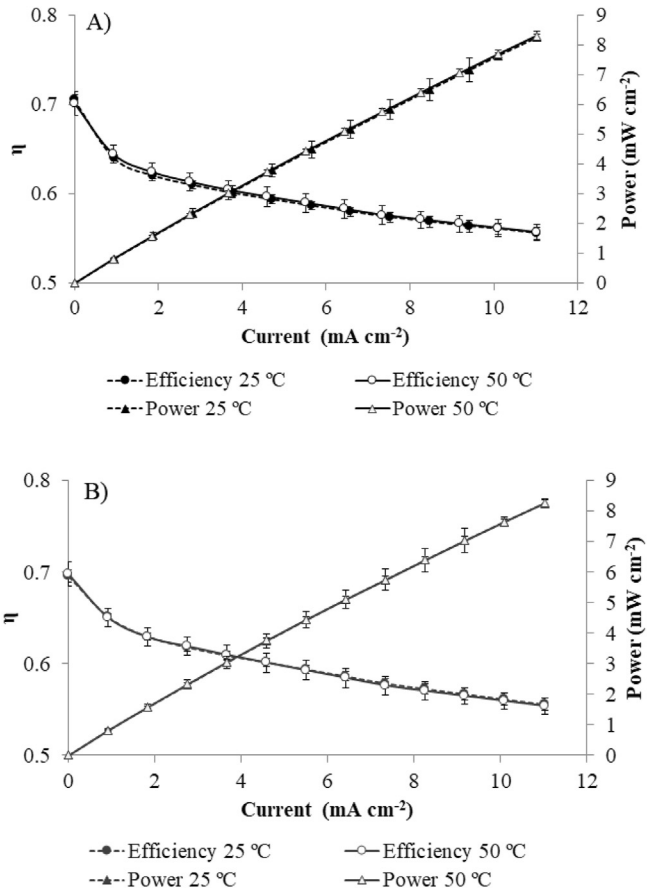

Fig. 9. Representation of the fuel cell efficiency data versus current and power for the lab-scale fuel cell operated with: A) bioH_2 produced during the operation of the continuous stirred-tank reactor (CSTR); B) commercial H_2.

any type of temperature control, possibly counteracting the effect of the higher gas temperature. Moreover, the PEMFC unit was employed within the architecture of a single cell and not as a stack of cells. With this design the heat generated in the device is not enough to maintain a high temperature within the electrochemical energy generator. As it is, the analysis of the results does not indicate any advantage associated with the use of 50 °C as the operational temperature. Comparisons between Fig. 8A and B revealed no significant statistical difference between the type of fuel, i.e., the performance of the PEMFC did not vary with the origin of the gas. This result is indicative of the absence of serious contaminants in the bioH_2, particularly of CO and H_2S which are often produced in other biological systems, such as, for example, biogas production (Rahman et al., 2016). The removal of the CO_2 sequestration stage, theoretically, should have no influence on the performance of the described PEMFC as CO_2 is not considered a contaminant to the membrane, nor a serious poison to the catalysts. Fig. 9A and B depict the variation of the fuel cell efficiency according to the type of gas and operational temperature and, as previously observed, there were no significant differences for the considered variables. To avoid unnecessary energy expenditures associated with the temperature increase, 25 °C was elected as the appropriate operational temperature. In this condition, the efficiency registered varied between 50 and 70%, attaining its minimum value at maximum power (Fig. 9). The experimental data was used to quantify the ratio between power and H_2 input flow, 1.7 W L^{-1} h^{-1}. This value is consistent with literature values such as 1.86 W L^{-1} h^{-1} obtained by Rahman et al. (2016).

3.3. Process scale-up and system comparison

The integrated conversion systems proposed were dimensioned according to the specifications of the waste biomass feed, i.e., the facility will need to process 35000 t of organic waste per year (defined as FU, section 2.5.). The energy consumption pattern was considered to be the same for all analysed scenarios for four of the five unitary operations: grinding/mashing, fermentation, gas stripping and centrifugation. Only Sc#1 analysed the impact of the stage of contamination control (microwave) when performed at the industrial level. Results of the energy consumption per process stage analysis are depicted in Table 7.

The intensive energy stages are temperature related, such as the microwave stage for contamination control and the fermentative stage, which requires strict temperature control. In fact, the comparison between Sc#1 and Sc#2 indicated that the microwave pretreatment stage was the critical main point of the overall process. The energy consumption in Sc#1 reached a maximum of 11391.5 MWh y^{-1}, which is approximately 3.2 times higher to that used for reference (3594 MWh y^{-1} in Fig. 4, section 2.6.). This situation can potentially be avoided if the microwave pretreatment is undertaken at household level as suggested in a previous iteration of the system (Ortigueira et al., 2019a). When this change was considered, there was a 53.3% increase in energy consumption compared with the reference system. Table 8 registers the inventory formulated for both the reference and alternative systems in accordance to the defined FU.

The "Valorsul" biological treatment reference process is based on the anaerobic digestion of the biomass into biogas and compost. Biogas is burned within a combined heat and power unit (CHP) to produce electricity and heat for the process. Therefore, the main products considered were electricity and compost, and the only input accounted for was electricity (Valorsul, 2018). Conversely, the proposed alternative systems relied heavily upon different byproducts to support the viability of the process, particularly the organic acids obtained in the fermentation (butyric, acetic, formic and lactic acid) which have considerable importance in both the chemical and pharmaceutical industries. Through the quantification of the CO_{2eq} parameter, the contribution of each input and output was associated with its GWP. The GWP data were calculated according to emission factors obtained from the average minimum and maximum emission factors available in literature and specialised databases (Table 4, section 2.7.). Fig. 10 depicts the GWP potential of the various scenarios considered as alternative valorisation processes, taking into consideration the various contributions per input and output (credits (−) or burdens (+)). It serves the purpose of identifying the stages of highest CO_{2eq} contribution. Fig. 11 compares the quantified GWP for the selected scenarios according to the supplied electricity generation mix: current and low-renewables contribution.Figure 11

The default condition (Sc#1) implied the use of the defined media described in section 2.2, particularly the use of phosphates as buffer and ammonium chloride as nitrogen source and both

Table 7
Direct energy consumption of the alternative valorisation system (Scenario Sc#1 - default).

Stage	Energy (MWh y^{-1})
1. Grinding/mashing	38.8
2. Microwaving	5880.0
3. Fermentation	1830.1
4. Gas stripping	0.0
5. Centrifugation	3642.5
Total	11391.5

Table 8
Inventory for the reference and alternative systems, per functional unit (FU): Sc#1. Default; Sc#2. Default without microwave pretreatment; Sc#3. Sludge recirculation to H_2; Sc#4. Sludge recirculation to electricity; Sc#5. Sludge recirculation to H_2, without CO_2 sequestration; Sc#6. Sludge recirculation to electricity, without CO_2 sequestration.

		Reference biological treatment	Scenario					
			1	2	3	4	5	6
Inputs (t y^{-1})	**Biomass input (FU)**	35000	35000	35000	35000	35000	35000	35000
	Iron sulphate	–	1114	1114	1114	1114	1114	1114
	Sodium hydroxide	–	4159	4159	4159	4159	1359	1359
	Ammonium chloride[a]	–	4076	4076	15	15	15	15
	Cysteine-HCl[a]	–	190	190	190	190	190	190
	Disodium phosphate[a]	–	2962	2962	2962	2962	2962	2962
	Monosodium phosphate[a]	–	2391	2391	2391	2391	2391	2391
Inputs (MWh y^{-1})	**Electricity**	3594	11392	5512	5512	5512	5512	5512
Outputs (t y^{-1})	**Hydrogen**	–	57	57	57	–	57	–
	Acetic acid	–	583	583	583	583	583	583
	Butyric acid	–	1340	1340	1340	1340	1340	1340
	Lactic acid	–	730	730	730	730	730	730
	Formic acid	–	393	393	393	393	393	393
	Sodium hydrogen carbonate	–	3710	3710	3710	3710	–	–
	Compost/sludge	669	9835	9835	–	–	–	–
	Carbon dioxide	6829	–	1540	–	–	–	–
Outputs (MWh y^{-1})	**Electricity**	9200	–	–	–	1078	–	1078

[a] Components of the minimum mineral medium (MMM).

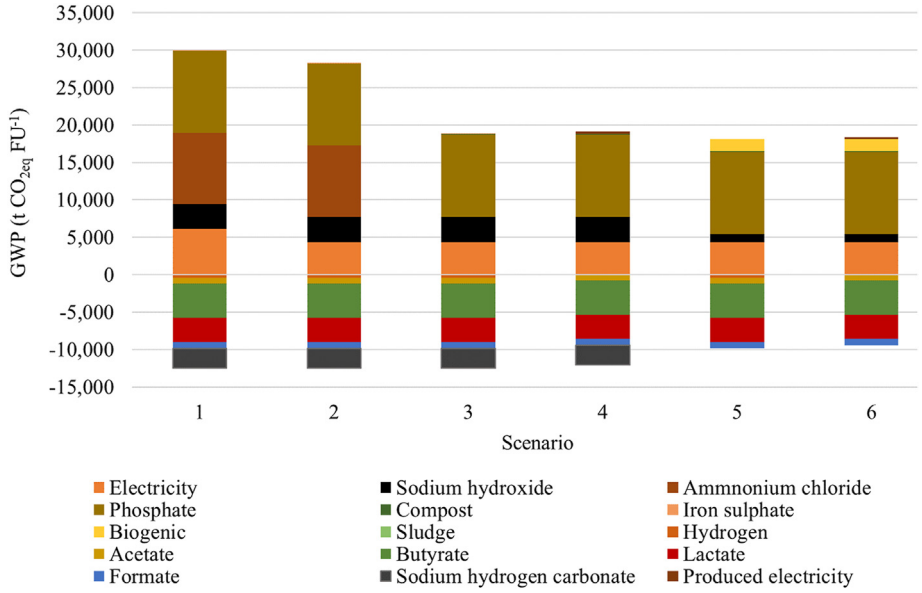

Fig. 10. Global warming potential (GWP) of the alternative valorisation systems according to the described scenarios, per FU: Sc#1. Default; Sc#2. Default without microwave pretreatment; Sc#3. Sludge recirculation to H_2; Sc#4. Sludge recirculation to electricity; Sc#5. Sludge recirculation to H_2, without CO_2 sequestration; Sc#6. Sludge recirculation to electricity, without CO_2 sequestration.

compounds have relatively high associated emissions. Nitrogen cannot be removed completely as it is a vital compound for cellular growth and this particular FW does not have enough nitrogen content for the optimal development of *C. butyricum* (Ortigueira et al., 2019a). It was postulated that the byproduct acidogenic sludge could be recirculated into the bioreactor and used as source of nitrogen (Ortigueira et al., 2019b). The application of this change to fermentation parameters decreased the GWP emissions by 64.3 and 63.8% in Sc#3 and Sc#4, respectively, and was considered the most advantageous condition. Conversely, the hypothesis of withdrawing the buffer solution is not ideal as the fermentation is highly dependent on pH for optimum results. The absence of a buffer leads to high variations in the pH value of the culture, caused by the fermentative acid production and the addition of NaOH solution for pH control. These variations can influence negatively the cellular viability. A previous study explored the effects of the replacement of a buffer solution by tap water and the removal of the nitrogen source on the fermentation of FW (Ortigueira et al., 2019a). It was concluded that none of these modifications prevented FW conversion, though the removal of both produced a negative impact in the fermentation performance. Nevertheless, further experiments must be undertaken to fully evaluate the need for a buffer solution and its effects, as sodium hydroxide is generally associated with high carbon emissions (Thannimalay et al., 2013). In the present work, NaOH was used for both CO_2 sequestration as well as pH control. The removal of the CO_2 capture step eliminates a secondary product – sodium hydrogen carbonate – while increasing the quantification of the biogenic CO_2 produced during fermentation. Overall, the impact of NaOH withdrawal considered both in Sc#5 and Sc#6 was negative, increasing the GWP values by

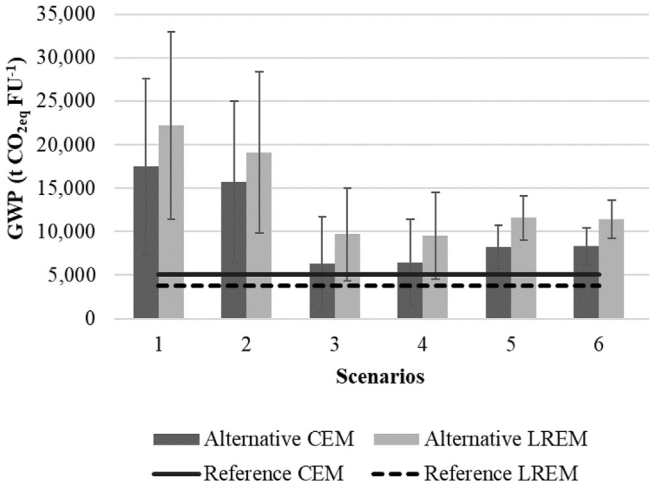

Fig. 11. Global warming potential (GWP) calculated for the reference and alternative scenarios considering the electricity mix: current electricity mix (CEM) and low-renewable electricity mix (LREM).

approximately 30%. The last analysis compared the effects caused by the inclusion of a final conversion of H_2 to electricity in a fuel cell (Sc#3 *vs* Sc#4 and Sc#5 *vs* Sc#6). The comparison between Sc#3 and Sc#4 indicated a 2.3% increase in GWP when electricity was considered the final product. When the emissions of the electricity mix were not considered to be from renewable origin, i.e., 524 kg CO_{2eq} MWh^{-1}, Sc#4 performed more favourably, reaching a maximum GWP decrease of 1.9% compared to Sc#3.

The reference conversion system considered electricity as its main product. Therefore, the increase of the non-renewable fraction in the electricity mix resulted in a 25% reduction of the overall GWP value. Conversely, the increase in emissions of the electricity mix impacted negatively in all the scenarios considered for the alternative systems due to the emission input increase. The analysis led to the conclusion that the removal of NH_4Cl from the fermentation media (Sc#3) reduced greatly the GWP value of the system. Taking into consideration the uncertainty of the GWP inputs, we obtained a range of GWP values for Sc#3 of 4290–14983 t of CO_{2eq}. Addressing the uncertainty is required in order to evaluate with precision whether the Sc#3 alternative would indeed generate a positive impact when compared to the reference.

4. Conclusions

The fermentation of FW by *C. butyricum* was undertaken successfully under non-sterile conditions in a CSTR. The predominance of the biocatalyst was favoured by the application of a microwave pretreatment to FW for substrate contamination control, and by operational settings that favoured *C. butyricum* activity, such as low HRT and adjustment of the optimum pH and temperature. During the 16 days of process time the average H_2 production remained stable at 6.1 ± 1.3 L H_2 L^{-1} d^{-1}, with an average composition of 95.8 ± 1.0% vol. of H_2 in the produced biogas and an average yield of 74.9 ± 15.8 L H_2 kg^{-1}_{VS}. The principal cometabolites produced were butyric and acetic acid, totalising 5.2 ± 0.8 g L^{-1} in the fermentate. The biogas produced in the CSTR was enriched in H_2 by CO_2 stripping, and fed to a PEMFC at two operational temperatures for electricity generation. No significant differences in the cell performance were recorded under all tested conditions, nor when compared to commercial H_2. The data obtained during the experimental procedure were used to model a process scale-up for electricity generation from biological H_2 produced from 35000 t of organic waste per year, and for the estimation of GWP values according to six scenarios. The best scenario (Sc#3), *i.e.* with the lower GWP value of 4290–14983 t of CO_{2eq}, was the one in which the fermentation nitrogen source was replaced by recycled DF-sludge. Future studies should focus on the implementation of a pilot scale reactor with possible suppression of the GWP-heavier inputs, as well as refining the GWP analysis to reduce uncertainty. Furthermore, analysis should be expanded to include additional environmental impact categories, such as the water footprint based on the ISO 14046:2014, among others.

Funding sources and acknowledgments

The authors would like to acknowledge the financial support by FCT through the projects UIDB/50019/2020 – IDL and UIDB/00100/2020 – CQE and the support from the Biomass and Bioenergy Research Infrastructure (BBRI)- LISBOA-01-0145-FEDER-022059, Operational Programme for Competitiveness and Internationalisation (PORTUGAL 2020), Lisbon Portugal Regional Operational Programme (Lisboa 2020) and North Portugal Regional Operational Programme (Norte 2020) under the Portugal 2020 Partnership Agreement, through the European Regional Development Fund (ERDF). This work was an integrated part of the project CONVERTE, supported by POSEUR (POSEUR-01-1001-FC-000001) under the PORTUGAL 2020 Partnership Agreement. Joana Ortigueira acknowledges FCT for the PhD grant SFRH/BD/107780/2015. The authors would also like to thank the technical assistance of Céu Penedo (biomass characterisation) and Luís Ramalho (GC analysis). Furthermore, the authors would like to thank Tania Chen Barbachano (BA & MA) for proofreading and editing the present manuscript.

CRediT authorship contribution statement

Joana Ortigueira: Investigation, Formal analysis, Writing - original draft. **Marta Pacheco:** Investigation. **Maria Ascensão Trancoso:** Formal analysis. **Pedro Farrancha:** Investigation. **Jorge Correia:** Investigation, Supervision. **Carla Silva:** Formal analysis, Supervision. **Patrícia Moura:** Investigation, Writing - original draft, Writing - review & editing, Conceptualization, Supervision.

Declaration of competing interest

The authors declare that they have no known competing financial interests or personal relationships that could have appeared to influence the work reported in this paper.

References

Alexandropoulou, M., Antonopoulou, G., Trably, E., Carrere, H., Lyberatos, G., 2018. Continuous biohydrogen production from a food industry waste: influence of operational parameters and microbial community analysis. J. Clean. Prod. 174, 1054–1063. https://doi.org/10.1016/j.jclepro.2017.11.078.

Algapani, D.E., Qiao, W., Ricci, M., Bianchi, D., M Wandera, S., Adani, F., Dong, R., 2019. Bio-hydrogen and bio-methane production from food waste in a two-stage anaerobic digestion process with digestate recirculation. Renew. Energy 130, 1108–1115. https://doi.org/10.1016/j.renene.2018.08.079.

Bazyar Lakeh, A.A., Azizi, A., Hosseini Koupaie, E., Bekmuradov, V., Hafez, H., Elbeshbishy, E., 2019. A comprehensive study for characteristics, acidogenic fermentation, and anaerobic digestion of source separated organics. J. Clean. Prod. 228, 73–85. https://doi.org/10.1016/j.jclepro.2019.04.223.

Cetinkaya, E., Dincer, I., Naterer, G.F., 2012. Life cycle assessment of various hydrogen production methods. Int. J. Hydrogen Energy 37, 2071–2080. https://doi.org/10.1016/j.ijhydene.2011.10.064.

ChemicalBook, 2016. ChemicalBook [WWW Document]. URL. https://www.chemicalbook.com/ProductIndex_EN.aspx. accessed 12.1.19.

Chen, W.M., Tseng, Z.J., Lee, K.S., Chang, J.S., 2005. Fermentative hydrogen production with CGS5 isolated from anaerobic sewage sludge. Int. J. Hydrogen Energy 30, 1063–1070. https://doi.org/10.1016/j.ijhydene.2004.09.008.

Cheng, J., Zhu, C., Zhu, J., Jing, X., Kong, F., Zhang, C., 2020. Effects of waste rusted

iron shavings on enhancing anaerobic digestion of food wastes and municipal sludge. J. Clean. Prod. 242, 118195. https://doi.org/10.1016/j.jclepro.2019.118195.
Cheng, X., Shi, Z., Glass, N., Zhang, L., Zhang, J., Song, D., Liu, Z.S., Wang, H., Shen, J., 2007. A review of PEM hydrogen fuel cell contamination: impacts, mechanisms, and mitigation. J. Power Sources 165, 739–756. https://doi.org/10.1016/j.jpowsour.2006.12.012.
Collet, P., Hélias Arnaud, A., Lardon, L., Ras, M., Goy, R.A., Steyer, J.P., 2011. Life-cycle assessment of microalgae culture coupled to biogas production. Bioresour. Technol. 102, 207–214. https://doi.org/10.1016/j.biortech.2010.06.154.
Corrado, S., Sala, S., 2018. Food waste accounting along global and European food supply chains: state of the art and outlook. Waste Manag. 79, 120–131. https://doi.org/10.1016/j.wasman.2018.07.032.
De Gioannis, G., Muntoni, A., Polettini, A., Pomi, R., Spiga, D., 2017. Energy recovery from one- and two-stage anaerobic digestion of food waste. Waste Manag. 68, 595–602. https://doi.org/10.1016/j.wasman.2017.06.013.
De Marco, I., Riemma, S., Iannone, R., 2018. Uncertainty of input parameters and sensitivity analysis in life cycle assessment: an Italian processed tomato product. J. Clean. Prod. 177, 315–325. https://doi.org/10.1016/j.jclepro.2017.12.258.
De Menna, F., Dietershagen, J., Loubiere, M., Vittuari, M., 2018. Life cycle costing of food waste: a review of methodological approaches. Waste Manag. 73, 1–13. https://doi.org/10.1016/j.wasman.2017.12.032.
Ecoinvent database, 2016. Ecoinvent V3 Database.
European Commission Joint Research Centre, EUCAR, Concawe, 2014. WTT JRC database [WWW Document]. WTT JRC database. URL. https://ec.europa.eu/jrc/en/jec.
European Environmental Agency, 2019. No title [WWW Document]. URL. https://www.eea.europa.eu/. accessed 9.20.19.
European Parliament and Council, 2019. Commission Delegated Decision (EU) Supplementing Directive 2008/98/EC of the European Parliament and of the Council as Regards a Common Methodology and Minimum Quality Requirements for the Uniform Measurement of Levels of Food Waste.
European Parliament and Council, 2018. Directive (EU) 2018/851 of the European parliament and of the Council of 30 may 2018 amending directive 2008/98/EC on waste. Off. J. Eur. Union 109–140. https://doi.org/10.1023/A:1009932427938.
Falconer, R.E., Haltas, I., Varga, L., Forbes, P.J., Abdel-Aal, M., Panayotov, N., 2020. Anaerobic Digestion of food waste: eliciting sustainable water-energy-food nexus practices with Agent Based Modelling and visual analytics. J. Clean. Prod. 255, 120060. https://doi.org/10.1016/j.jclepro.2020.120060.
Gharehpetian, G.B., Mousavi Agah, S.M., Abdi, H., Rasouli Nezhad, R., Salehimaleh, M., 2017. Fuel Cells, Distributed Generation Systems. Butterworth-Heinemann. https://doi.org/10.1016/B978-0-12-804208-3.00005-4.
Harzevili, F.D., Hiligsmann, I.S., 2017. Microbial Fuels: Technologies and Applications, first ed. CRC Press, Taylor & Francis Group, Florida, USA.
Hervy, M., Evangelisti, S., Lettieri, P., Lee, K.Y., 2015. Life cycle assessment of nanocellulose-reinforced advanced fibre composites. Compos. Sci. Technol. 118, 154–162. https://doi.org/10.1016/j.compscitech.2015.08.024.
Horwitz, W., Latimer, G.W., 2005. A.O.A.C. Official methods of analysis. In: Association of the Official Analytical Chemists, eighteenth ed. A.O.A.C. International, Gaithersburg MD, USA.
Huang, J., Feng, H., Huang, L., Ying, X., Shen, D., Chen, T., Shen, X., Zhou, Y., Xu, Y., 2020. Continuous hydrogen production from food waste by anaerobic digestion (AD) coupled single-chamber microbial electrolysis cell (MEC) under negative pressure. Waste Manag. 103, 61–66. https://doi.org/10.1016/j.wasman.2019.12.015.
Kanchanasuta, S., Prommeenate, P., Boonapatcharone, N., Pisutpaisal, N., 2017. Stability of *Clostridium butyricum* in biohydrogen production from non-sterile food waste. Int. J. Hydrogen Energy 42, 3454–3465. https://doi.org/10.1016/j.ijhydene.2016.09.111.
Kehili, M., Schmidt, L.M., Reynolds, W., Zammel, A., Zetzl, C., Smirnova, I., Allouche, N., Sayadi, S., 2016. Biorefinery cascade processing for creating added value on tomato industrial by-products from Tunisia. Biotechnol. Biofuels 9, 1–12. https://doi.org/10.1186/s13068-016-0676-x.
Kirubakaran, A., Jain, S., Nema, R.K., 2009. A review on fuel cell technologies and power electronic interface. Renew. Sustain. Energy Rev. 13, 2430–2440. https://doi.org/10.1016/j.rser.2009.04.004.
Koroglu, E.O., Ozdemir, O.K., Ozkaya, B., Demir, A., 2019. An integrated system development including PEM fuel cell/biogas purification during acidogenic biohydrogen production from dairy wastewater. Int. J. Hydrogen Energy 44, 17297–17303. https://doi.org/10.1016/j.ijhydene.2019.01.291.
Kwan, T.H., Pleissner, D., Lau, K.Y., Venus, J., Pommeret, A., Lin, C.S.K., 2015. Techno-economic analysis of a food waste valorization process via microalgae cultivation and co-production of plasticizer, lactic acid and animal feed from algal biomass and food waste. Bioresour. Technol. 198, 292–299. https://doi.org/10.1016/j.biortech.2015.09.003.
Larminie, J., Lowry, J., 2012. Electric Vehicle Technology Explained, second ed. John Wiley & Sons, Inc., New Jersey, USA.
Lin, C.N., Wu, S.Y., Lee, K.S., Lin, P.J., Lin, C.Y., Chang, J.S., 2007. Integration of fermentative hydrogen process and fuel cell for on-line electricity generation. Int. J. Hydrogen Energy 32, 802–808. https://doi.org/10.1016/j.ijhydene.2006.09.047.
Lipinski, B., Hanson, C., Lomax, J., Kitinoja, L., Waite, R., Searchinger, T., 2013. Reducing food loss and waste. World Resour. Inst. 1–40.
Nishikawa, H., Sasou, H., Kurihara, R., Nakamura, S., Kano, A., Tanaka, K., Aoki, T., Ogami, Y., 2008. High fuel utilization operation of pure hydrogen fuel cells. Int. J. Hydrogen Energy 33, 6262–6269. https://doi.org/10.1016/j.ijhydene.2008.07.019.
Olatunde, G.A., Atungulu, G.G., Smith, D.L., 2017. One-pass drying of rough rice with an industrial 915 MHz microwave dryer: quality and energy use consideration. Biosyst. Eng. 155, 33–43. https://doi.org/10.1016/j.biosystemseng.2016.12.001.
Ortigueira, J., Alves, L., Gouveia, L., Moura, P., 2015. Third generation biohydrogen production by *Clostridium butyricum* and adapted mixed cultures from *Scenedesmus obliquus* microalga biomass. Fuel 153, 128–134. https://doi.org/10.1016/j.fuel.2015.02.093.
Ortigueira, J., Martins, L., Pacheco, M., Silva, C., Moura, P., 2019a. Improving the non-sterile food waste bioconversion to hydrogen by microwave pretreatment and bioaugmentation with *Clostridium butyricum*. Waste Manag. 88, 226–235. https://doi.org/10.1016/j.wasman.2019.03.021.
Ortigueira, J., Moura, P., Silva, C., 2019b. Dark fermentation sludge as nitrogen source for hydrogen production from food waste. In: Wastes: Solutions, Treatments and Opportunities III: Selected Papers from the 5th International Conference Wastes 2019, p. 301.
Panigrahi, S., Sharma, H.B., Dubey, B.K., 2020. Anaerobic co-digestion of food waste with pretreated yard waste: a comparative study of methane production, kinetic modeling and energy balance. J. Clean. Prod. 243, 118480. https://doi.org/10.1016/j.jclepro.2019.118480.
Pleissner, D., Lam, W.C., Sun, Z., Lin, C.S.K., 2013. Food waste as nutrient source in heterotrophic microalgae cultivation. Bioresour. Technol. 137, 139–146. https://doi.org/10.1016/j.biortech.2013.03.088.
Pleissner, D., Lau, K.Y., Zhang, C., Lin, C.S.K., 2015. Plasticizer and surfactant formation from food-waste- and algal biomass-derived lipids. ChemSusChem 8, 1686–1691. https://doi.org/10.1002/cssc.201402888.
Qin, Y., Li, L., Wu, J., Xiao, B., Hojo, T., Kubota, K., Cheng, J., Li, Y.Y., 2019. Co-production of biohydrogen and biomethane from food waste and paper waste via recirculated two-phase anaerobic digestion process: bioenergy yields and metabolic distribution. Bioresour. Technol. 276, 325–334. https://doi.org/10.1016/j.biortech.2019.01.004.
Rahman, S.N.A., Masdar, M.S., Rosli, M.I., Majlan, E.H., Husaini, T., Kamarudin, S.K., Daud, W.R.W., 2016. Overview biohydrogen technologies and application in fuel cell technology. Renew. Sustain. Energy Rev. 66, 137–162. https://doi.org/10.1016/j.rser.2016.07.047.
Ren, N., Guo, W., Liu, B., Cao, G., Ding, J., 2011. Biological hydrogen production by dark fermentation: challenges and prospects towards scaled-up production. Curr. Opin. Biotechnol. 22, 365–370. https://doi.org/10.1016/j.copbio.2011.04.022.
Rico, C., Montes, J.A., Lobo, A., 2020. Dry batch anaerobic digestion of food waste in a box-type reactor system: inoculum preparation and reactor performance. J. Clean. Prod. 251, 119751. https://doi.org/10.1016/j.jclepro.2019.119751.
Sánchez Maldonado, A.F., Mudge, E., Gänzle, M.G., Schieber, A., 2014. Extraction and fractionation of phenolic acids and glycoalkaloids from potato peels using acidified water/ethanol-based solvents. Food Res. Int. 65, 27–34. https://doi.org/10.1016/j.foodres.2014.06.018.
Sivagurunathan, P., Kumar, G., Bakonyi, P., Kim, S.-H., Kobayashi, T., Xu, K.Q., Lakner, G., Tóth, G., Nemestóthy, N., Bélafi-Bakó, K., 2016. A critical review on issues and overcoming strategies for the enhancement of dark fermentative hydrogen production in continuous systems. Int. J. Hydrogen Energy 1. https://doi.org/10.1016/j.ijhydene.2015.12.081.
Soda, S., Iwai, Y., Sei, K., Shimod, Y., Ike, M., 2010. Model analysis of energy consumption and greenhouse gas emissions of sewage sludge treatment systems with different processes and scales. Water Sci. Technol. 61, 365–373. https://doi.org/10.2166/wst.2010.827.
Stenmarck, Å., Jensen, C., Quested, T., Moates, G., Buksti, M., Cseh, B., Juul, S., Parry, A., Politano, A., Redlingshofer, B., Scherhaufer, S., Silvennoinen, K., Soethoudt, H., Zübert, C., Östergren, K., 2016. Estimates of European Food Waste Levels. Reducing Food Waste through Social Innovation. IVL Swedish Environmental Research Institute, Stockholm, Sweden (FUSIONS project). ISBN 978-91-88319-01-2.
Thannimalay, L., Yusoff, S., Zawawi, N.Z., 2013. Life cycle assessment of sodium hydroxide. Aust. J. Basic Appl. Sci 7, 421–431.
Valorsul, 2018. Relatório & contas 2018. Valorização e Tratamento de Resíduos Sólidos das Regiões de Lisboa e do Oeste. S.A., Lisboa.
Water Technology, 2012. UZOS South-West wastewater treatment plant annual data [WWW Document]. URL. https://www.winnipeg.ca/finance/findata/matmgt/documents/2012/682-2012/682-2012_Appendix_HWSTP_South_End_Plant_Process_Selection_Report/Appendix 7.pdf. accessed 1.11.19.
Yang, X., Lee, J.H., Yoo, H.Y., Shin, H.Y., Thapa, L.P., Park, C., Kim, S.W., 2014. Production of bioethanol and biodiesel using instant noodle waste. Bioproc. Biosyst. Eng. 37, 1627–1635. https://doi.org/10.1007/s00449-014-1135-3.
Youn, J.-H., Shin, H.-S., 2005. Comparative performance between temperature phased and conventional mesophilic two-phased processes in terms of anaerobically produced bioenergy from food waste. Waste Manag. Res. 23, 32–38. https://doi.org/10.1177/0734242X05049766.